Simple systematic synthesis of size-tunable covalent organophosphonitridic framework nano- and microspheres†

Paritosh Mohanty and Kai Landskron*

Received (in Montpellier, France) 2nd September 2009, Accepted 17th November 2009
First published as an Advance Article on the web 12th January 2010
DOI: 10.1039/b9nj00446g

Covalent organophosphonitridic framework nano- and microspheres were synthesized by a condensation reaction between hexachlorocyclotriphosphazene (PNC) and 3,3′-diaminobenzidine (DAB) in anhydrous dimethylformamide (DMF) at a temperature of 125 °C in the presence of polyvinyl pyrrolidone (PVP). The spheres were almost monodisperse and the diameter could be adjusted from 80 nm to 1.5 μm by varying the concentration of the reactants PNC and DAB. The spheres are thermally stable up to 480 °C in air and are completely oxidatively-depolymerized at 750 °C.

Introduction

Crystalline covalent organic frameworks are a rapidly emerging class of framework materials that are attractive candidates for applications in gas storage for separation due to their high crystallinity and surface area.[1–11] The field was created by the seminal work by Yaghi *et al*., who reported the dehydration reaction of 1,4-benzenediboronic acid to form its anhydride, as well as the condensation of 1,4-benzenediboronic acid with hexahydroxytriphenylene to form highly porous crystalline framework materials with high surface areas.[10] Most of the crystalline covalent organic frameworks known today are boronic acid esters and anhydrides. However, very recently, the first crystalline covalent organic frameworks of other compositions namely, organoborosilicates,[5] organocarbonitrides[11] and imine-linked covalent organic frameworks,[2] have been synthesized. Also, a range of amorphous covalent organic frameworks, dubbed hypercrosslinked polymers (HCP), have gained considerable attention recently.[12–19] Amorphous frameworks are particularly attractive from the standpoint of chemical stability because they can be easily constructed from bonds that cannot be easily reversibly formed and cleaved, a feature mandatory for crystallization.

We have recently started a research project targeting electron-rich, covalent, organophosphonitridic frameworks, in which electron-rich aromatic constituents, in particular, are able to interact with electron-poor molecules in a donor–acceptor fashion. These interactions could potentially be exploited for the separation of electron-poor Lewis acidic molecules, *e.g*. carbon dioxide, from other molecules. Aromatic molecules with multiple amino groups are known to be particularly electron-rich molecules. We chose 3,3′-diaminobenzidine (DAB), which carries overall four amino groups, because it appealed as a ditopic bridging organic linker in condensation reactions. In order to create a framework material, it is mandatory to interconnect a ditopic linker with a unit that is at least tritopic. We chose hexachlorocyclotriphosphazene (PNC) as a tritopic linker. PNC has a rigid nitridic P_3N_3 unit and is known to readily condense with *ortho*-functionalized benzenes such as catechol, 1,2-diaminobenzene, and 1,2-benzenedithiol.[20–22] The expected product represents a covalent organophosphonitridic framework according to Scheme 1. The expected electron-rich framework is expected to be amorphous yet very stable because it is entirely constructed of highly covalently bonded rigid cyclic units, exploiting the chelate effect between the P centers and the *ortho*-positioned amino groups.

Results and discussion

In order to produce the target product, we heated a mixture of 2.4 mmol of DAB and 0.8 mmol of PNC in 40 ml of DMF at 125 °C for 10 min. Within this short reaction time, a white suspension was obtained. The obtained product (sample A) was subjected to SEM to investigate its structure and morphology. Surprisingly, spherical particles were revealed by SEM. The sizes of the spheres ranged from 200 nm to 2 μm,

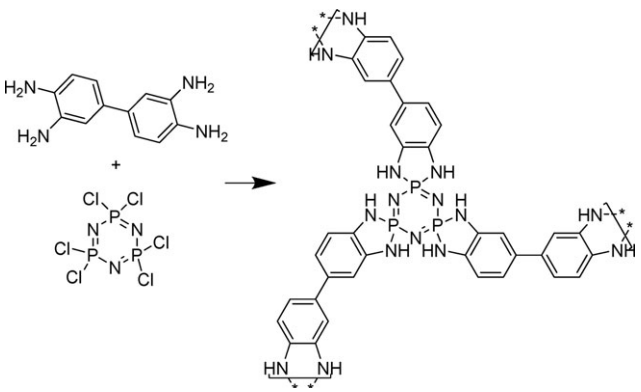

Scheme 1 Reaction scheme for the synthesis of nano- and microspheres.

Department of Chemistry, Lehigh University, Bethlehem, Pennsylvania-18015, USA. E-mail: kal205@lehigh.edu; Fax: +1 610-758-6536; Tel: +1 610-758-5788

† Electronic supplementary information (ESI) available: XRD and SAED patterns, DLS spectra, TGA/DTG thermograms, and an additional SEM image. See DOI: 10.1039/b9nj00446g

as shown in Fig. 1(a). The obtained product was subjected to powder X-ray diffraction and found to be X-ray amorphous (Fig. S1†). This result was expected, as the P–N bonds formed during the condensation reaction are very inert, prohibiting crystallization. A representative selected area electron diffraction pattern (SAED pattern) is shown in Fig. S2,† which confirms that the samples are amorphous in nature. The composition of the sample was studied by elemental analysis. The elemental composition of the sample gave a ratio of $PN_{2.67}C_{7.3}H_{10.1}Cl_{0.37}O_{2.18}$. Assuming a fully condensed product, the theoretical ratios of the elements are $PN_{2.33}C_4H_{2.67}$. An excess of $N_{0.27}C_{3.3}H_{7.43}Cl_{0.37}O_{2.18}$ was observed, indicating that the product is not fully condensed. This was corroborated by the presence of small amounts of Cl, which indicates that the PNC may not have fully reacted with the amines. However, ionic chloride is also plausible as the Cl source because evolved HCl during the reaction process may have protonated free terminal amino groups in the framework. The latter scenario appears to be more likely because the amine was used in excess in the synthesis. The presence of the excess C, H and N can also be attributed to the terminal aromatic amines, which reduces the degree of condensation.

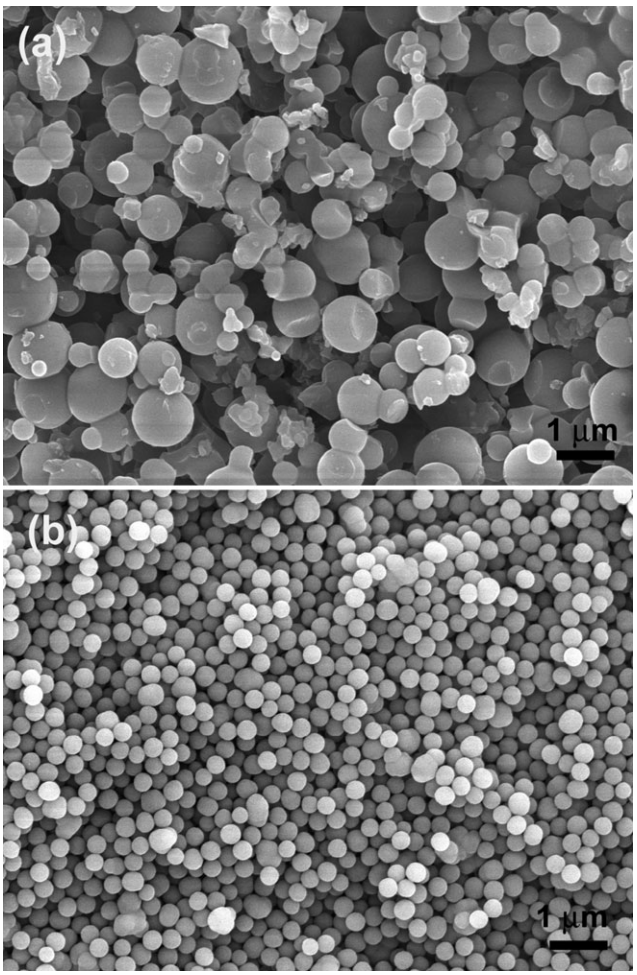

Fig. 1 SEM images of spheres produced: (a) without PVP (sample A) and (b) with the addition of 50 mg of PVP to the reaction mixture of 2.4 mmol of DAB and 0.8 mmol of PNC in 40 ml of DMF (sample C).

The presence of O can be attributed to DMF occlusion and possibly water. The presence of occluded DMF was confirmed by ^{13}C solid state MAS-NMR and thermogravimetric analysis (TGA).

Fig. 2(a) shows the ^{13}C MAS-NMR spectrum of the product. The observation of five signals at 110, 116, 124, 131, and 139 ppm confirms that the aromatic ring was incorporated into the material during the synthesis. The observed shifts match well with the shifts for the DAB molecule. Three additional signals observed at 35, 41, and 155 ppm can be attributed to occluded DMF, which is consistent with the observation of higher C, N and H contents, and the presence of O, in the elemental analysis. The material was further investigated by ^{31}P solid state MAS-NMR, showing a strong broad signal at 17 ppm with a shoulder at 25 ppm in Fig. 2(b). The results confirm the presence of phosphorus in the material and corroborate the results from the elemental analysis. Chemical shifts at 17 and 25 ppm are typical for frameworks composed of PN_4 tetrahedra.[20,21] The observation of two chemical shifts at similar values indicates that two structurally different environments for the P atoms in the framework are present. These may stem from P atoms surrounded by bridging and terminal DAB units, respectively. The presence of small amounts of Cl observed in the elemental analysis suggests that P–Cl units may also contribute to these signals. However, Cl could also result from the hydrochlorides of terminal amino groups in the framework, which may also slightly influence the ^{31}P NMR chemical shift. The presence of terminal amino groups in the framework is plausible considering that the DAB was used in excess in the synthesis, and the fact that C, H and N are found in excess by elemental analysis. Covalent organic frameworks often form porous structures due the rigidity of their building blocks and highly directional bonding. Therefore, we probed the porosity using N_2 and CO_2 sorption techniques. Sample A did not show any appreciable surface area and also did not adsorb noteworthy amounts of CO_2, indicating that either a non-porous structure or a structure with non-accessible closed pores is present. The results indicate that the produced material is highly interpenetrated and/or oligomeric, which explains the absence of a significant degree of porosity.

The thermal behavior of the sample A was studied by TGA/DTG (Fig. 3) in air. A mass loss of ~20% below 250 °C was observed. The mass loss occurs in two steps, most likely due to the desorption of water (100 °C) and occluded DMF (200–250 °C). A similar mass loss of ~20% was observed below 250 °C when the TGA/DTG was studied in a nitrogen atmosphere (Fig. S3†). This confirms that the mass loss is due to the desorption of adsorbed water and occluded solvent rather than any decomposition of the product. Remarkably, the material is thermally stable up to a temperature of 480 °C in air. In nitrogen, a gradual mass loss is observed from 500 °C that is likely to be associated with carbonization of the organic groups and the formation of a purely inorganic P–N framework. At 700 °C in nitrogen, a sharp mass loss occurs due to the depolymerization of the P–N framework. The mass loss above 480 °C in air takes place in two steps, which can clearly be seen in the DTG thermogram. The first step can be attributed to the oxidation of organic groups in the material. This was further

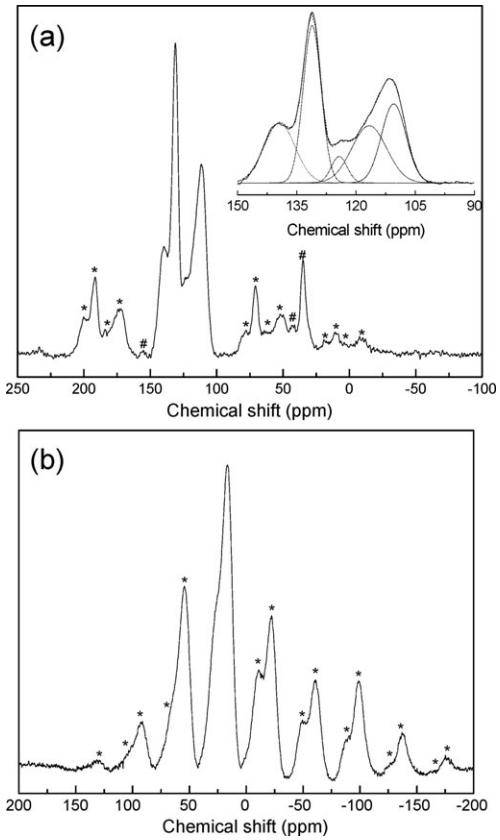

Fig. 2 (a) The ^{13}C MAS-NMR spectrum and (b) the ^{31}P MAS-NMR spectrum of sample A (* = rotational side bands; # signal from DMF).

confirmed due to the absence of this step when the thermal analysis was carried out in a nitrogen atmosphere. The second step can be attributed to the oxidation of the phosphazene component, which was complete at 750 °C in air. By comparison, this decomposition is complete at a higher temperature of 830 °C in a nitrogen atmosphere, which is typical for P–N materials.[23,24] This property is unique for a material containing inorganic building blocks. Complete combustion into volatile species (without leaving a non-volatile residue) is otherwise only possible for entirely organic systems. Thus, the spheres could potentially be used as template for making other functional nano or microstructured materials.

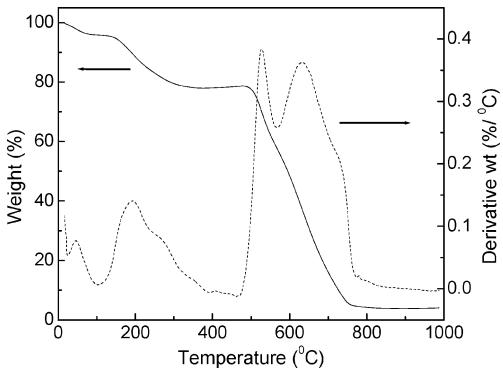

Fig. 3 TGA/DTG thermogram of the sample A in air.

The large size distribution of the obtained spheres prompted us to modify the reaction conditions in order to obtain spheres with a higher monodispersity. PVP has been used for controlling the shape and size of metal, metal oxide, and polymer spheres.[25–28] On adding 200 mg (0.0034 mmol) of PVP to the DAB/PNC reaction mixture in DMF, almost monodisperse spherical particles were observed with a size of ~600 nm, as shown by SEM (Fig. 1(b)). We further varied the concentration of the reactants systematically by keeping the DMF and PVP concentrations constant (samples B to G) to investigate whether the spheres could be obtained with different sizes. It was observed that there is a regular decrease in the size of the nanospheres upon decreasing the concentration of the reactants. Fig. 4 shows SEM images of spheres of different sizes obtained at different concentrations of reactants. Spheres with a size ~1.5 μm (Fig. 4(a)) were observed when 4.8 mmol of DAB was reacted with 1.6 mmol of PNC with a fixed amount of PVP (0.0034 mmol) and DMF (40 ml). Details of the experimental conditions are summarized in Table 1. The smallest nanospheres (sample G) were observed when 0.3 mmol of DAB was reacted with 0.1 mmol of PNC (Fig. 4(f)). In an attempt to decrease the size of the spheres, we further decreased the concentration of the reactants, but no precipitate was observed after the reaction time of 10 min. This may be explained by the fact that the polycondensation products are small enough in size to stay dissolved in solution. However, agglomerated spherical particles were observed on increasing the reaction time from 10 to 30 min (see ESI, Fig. S4†), which shows that the polycondensation process also takes place under these conditions. However, the size of the particles could no longer be easily controlled at this concentration.

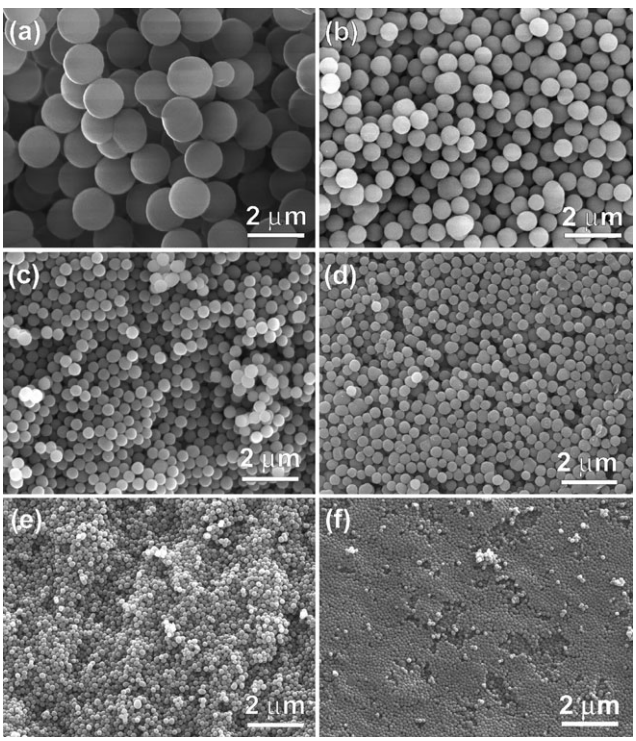

Fig. 4 SEM images of the organophosphonitridic spheres (samples B–G) obtained at different concentrations of PNC and DAB.

Table 1 Relationship between the reaction conditions and sphere diameters.

Sample	DAB/mmol	PNC/mmol	PVP/mmol	DMF/ml	R_h/nm	Diameter by SEM and TEM/nm
A	2.4	0.8	0	40	—	200–2000
B	4.8	1.6	0.0034	40	—	1500
C	2.4	0.8	0.0034	40	317	600
D	1.6	0.53	0.0034	40	250	450
E	1.2	0.4	0.0034	40	200	380
F	0.6	0.2	0.0034	40	82	160
G	0.3	0.1	0.0034	40	75	80

The spheres were further studied by TEM and SAED in order to confirm the sizes obtained by SEM, probe the texture inside the spheres and determine their crystallinity. Fig. 5 shows TEM images of the spheres synthesized at different concentrations of reactants. The sizes of the spheres are consistent with the values obtained from the SEM images. No texture could be found, which indicates that the spheres are non-porous and of homogeneous density. SAED did not indicate any crystallinity. The dependency of the sphere size on the concentration of the reactants is summarized in Fig. 6.

The dynamic light scattering (DLS) of the specimens was further studied to probe their aggregation behavior in solution. The DLS spectra of the specimens (C to G) at various concentrations measured at a scattering angle of 90° are shown in Fig. S5.† In each of the spectra, a sharp peak for the hydrodynamic radius (R_h) was obtained by CONTIN analysis of the obtained spectrum. This confirms the narrow particle size distribution and monodispersity of the specimens. The results show that the spheres can be dispersed in solution without a significant degree of aggregation. The size of the nanospheres measured by TEM and SEM are comparable with the R_h obtained by DLS, as summarized in Table 1. The R_h observed by DLS is somewhat larger than the actual radius observed by SEM and TEM analysis. Such an effect was previously observed for silica nanospheres.[29] It can be understood by considering that solvation effects increase the actual radius of the spherical object moving through a solution. Swelling effects can further contribute to the hydrodynamic radius. The effect is by far the strongest in the smallest nanospheres (sample G). This is plausible because swelling and solvation effects are expected to make a much larger contribution when the actual particle size is very small. Furthermore, we have measured the DLS of the specimens at various angles of incident light. A spectrum of a representative sample (sample F) is shown in Fig. S6.† The R_h of the specimen is not angle dependent, which further confirms the spherical nature of the particles. The spheres of samples A and B could not be measured because of their sizes, which are beyond the scope of the technique.

We further investigated the optical properties of the nanospheres by using a combination of UV-vis and photoluminescence (PL) spectroscopy. The optical properties of the specimens (samples A, E, F and G) were studied by dispersing the nanospheres ultrasonically in an aqueous solution. Fig. 7(a) shows the UV-vis spectra of nanospheres of varying size. Two absorption peaks at around 220 and 290 nm were

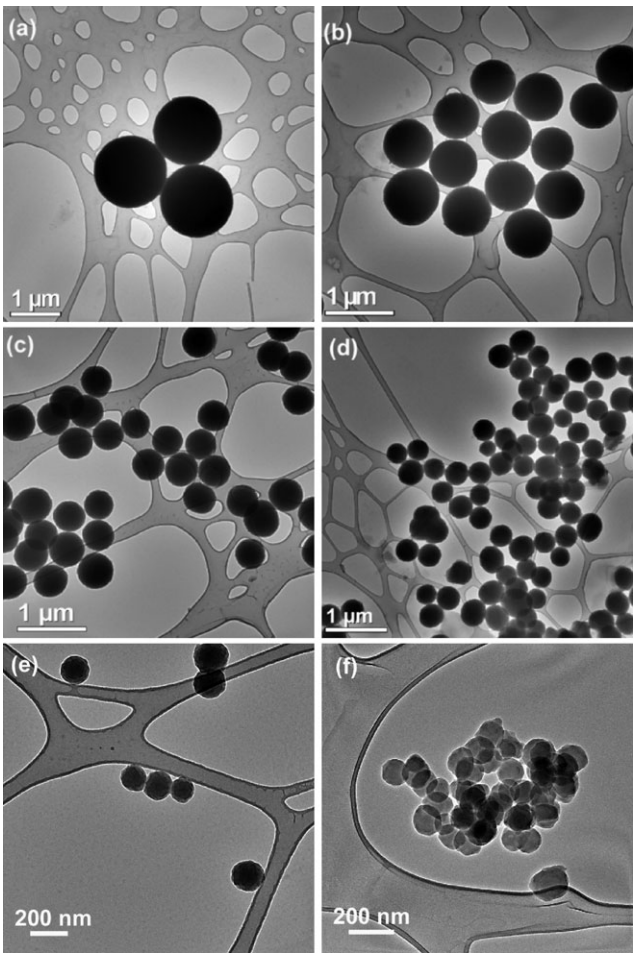

Fig. 5 TEM images of the organophosphonitridic spheres (samples B–G) obtained at different concentrations of PNC and DAB.

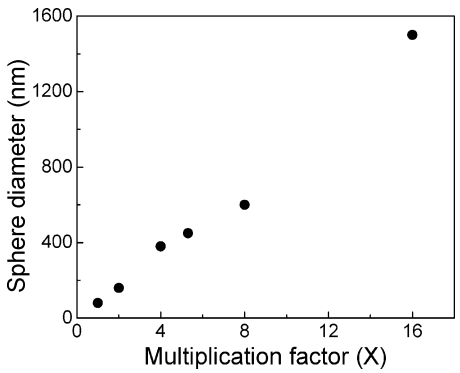

Fig. 6 Particle size *vs.* concentration of PNC and DAB; concentration = X (0.1 mmol of PNC + 0.3 mmol of DAB) at fixed amount of PVP (200 mg) and DMF (40 ml).

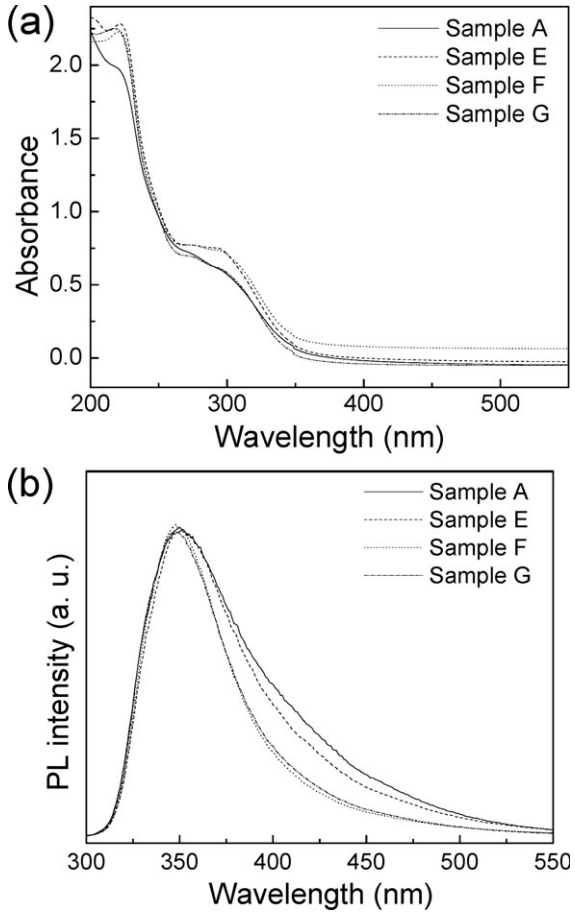

Fig. 7 (a) UV-vis and (b) PL spectra of samples A, E, F and G.

observed for all the samples. These absorption peaks can be attributed to the biphenyl amines. Such absorption was observed for *ortho*-, *meta*- and *para*-aminobiphenyl in the range of 220 to 283 nm, depending on the position of the amino group as well as the solvents used.[30] For the pure biphenyl, this absorption peak was observed at around 248 nm.[30]

The PL spectra of the samples (Fig. 7(b)) show a broad emission peak at 350 nm. Such an emission peak has been observed for aminobiphenyls and diaminobiphenyls.[30,31] The peak position doesn't change appreciably with the changing sphere size; however, the half peak width increases with increasing sphere size.

A question is: what drives the formation of the uniform spherical particles? An explanation may be an analogy to the growth of silica spheres, which form due to a specific charge density at the growing silica framework.[32] The charges prevent the particles from agglomerating and intergrowing. The particles adopt a spherical shape in order to minimize their surface area. By analogy, organonitride sphere formation may also be driven by charges at the growing framework because the HCl by-product can protonate N atoms, most likely the most basic free amino groups of the terminal organic DAB units. At a certain sphere size, which depends on the concentration of the reactants, PVP interacts significantly with the growing spheres, thereby coating them with PVP. The PVP-coated spheres are not able to grow further, resulting in a uniform sphere size.

Conclusions

In conclusion, we have prepared size-tunable covalent organophosphonitridic framework nano and microspheres by simple condensation reactions between 3,3′-diaminobenzidine and hexachlorocyclotriphosphazene in DMF. Their size could be controlled over more than one order of magnitude (80 nm to 1.5 μm) simply by varying the concentration of the reactants. The spheres are very stable in air (480 °C) but completely combustible into volatile molecular species (at 750 °C), which is a unique property for an inorganic–organic hybrid material.

Experimental section

Materials

Hexachlorocyclotriphosphazene (PNC): Alfa Aesar, 98%. 3,3′-Diaminobenzidine (DAB): AK Scientific, 99%. Anhydrous *N*,*N*-dimethyl formamide (DMF): Acros Organics, 99.8%. Polyvinyl pyrrolidone (PVP): Alfa Aesar (average molecular weight 58 000).

Synthesis of nano- and microspheres

In a typical synthesis, about 2.4 mmol of DAB was dissolved in 20 ml of DMF in a flask, and in another flask 0.8 mmol of PNC was dissolved in 20 ml of DMF. The PNC solution was added dropwise to the DAB solution at room temperature. The resulting solution was stirred for 10 min at RT to form a homogeneous solution. It was then heated at a temperature of 125 °C with vigorous stirring. A precipitate started to form as soon as 3 to 5 min, and the experiment was continued for 10 min under stirring conditions. The sample was cooled down to room temperature and the solid powders were collected by centrifugation. All of the experiments were carried out in a nitrogen atmosphere using a Schlenk apparatus. For the samples synthesized using PVP, the reactants were added to the fixed amount of the DMF/PVP solution.

Measurements

The formation of the nano and microspheres, and their optical properties and compositions were studied by scanning electron microscopy (SEM), transmission electron microscopy (TEM), X-ray diffraction (XRD), UV-Vis and photoluminescence (PL) spectroscopy, and elemental analysis. SEM images of the specimens were taken using a Hitachi S-4300 SEM. TEM images were taken on a JEOL JEM-2000 electron microscope operating at 200 kV. Samples for TEM analysis were prepared by dispersing the particles in an organic solvent and dropping a small volume of it onto a carbon-coated copper grid. X-ray diffraction was carried out using a Rigaku Rotaflex diffractometer with a Cu-K_α radiation source (λ = 0.15405 nm). Elemental analysis of a representative sample was carried out by Fa. Pascher (Remagen, Germany). TGA was carried out using a TA TGA 2950 instrument at a heating rate of 10 °C min^{-1}. DLS spectra of the specimens were taken using a BI-9000 AT

multi-channel digital correlator to measure the intensity–intensity time correlation function. The constrained regularized CONTIN method was used to analyze the field correlation function $g(\tau)$ and to obtain the characteristic line width Γ. The hydrodynamic radius (R_h) of the nanospheres can be calculated *via* the Stokes–Einstein equation, $R_h = kT/(6\pi\eta D)$, where k is the Boltzmann constant and η is the viscosity of the solvent at temperature T. ^{13}C NMR spectra were obtained at 75.468 MHz on a General Electric NMR Instrument model GN-300 equipped with a Doty Scientific 7 mm MAS probe. One pulse spectra were measured with a 1.0 μs pulse length (corresponding to a 20° tip angle) and a relaxation delay of 8 s for 6000 to 29 000 acquisitions, while typically spinning at 5.0 kHz. Proton decoupling during the 40 ms acquisition time was performed using a continuous 70 kHz radio frequency field of 300.107 MHz. The time domain signal was conditioned with a Gaussian line-broadening function equivalent to 50 Hz and one zero-fill prior to Fourier transformation. ^{31}P NMR spectra were obtained using the same equipment but with the following parameter changes: a spectrometer frequency of 121.485 MHz, relaxation delays of 20 to 200 s, the number of transients varied from 128 to 3600, a spinning speed 4.5 to 5 kHz, a few spectra had a total acquisition time of only 20 ms, and the line broadening was a Gaussian function equivalent to either 25 or 50 Hz in the frequency domain. ^{13}C NMR chemical shifts were referenced to the downfield line of adamantine at 38.55 ppm, and for ^{31}P NMR, the chemical shift of 85% H_3PO_4 was set to zero using external reference standards. UV-vis spectra of the samples were acquired on a Cary Eclipse 500 UV-Vis spectrophotometer. Photoluminescence (PL) spectra of specimens were obtained using a Cary Eclipse 500 fluorescence spectrophotometer. PL spectra were taken by exciting the samples at λ_{ext} = 280 nm.

Acknowledgements

This work was supported by Lehigh University start-up funds and faculty grants. Dr. James E. Roberts is gratefully acknowledged for MAS-NMR measurements. We further thank Dr. Chris Kiely and Dr. Dave Ackland for generously supporting our TEM investigations. Dr. G. Slade Cargill is gratefully acknowledged for supporting our X-ray diffraction experiments. We acknowledge Mr. Wade H. Bailey for supporting our thermal analysis experiments.

References

1 H. Furukawa and O. Yaghi, *J. Am. Chem. Soc.*, 2009, **131**, 8875.
2 F. Uribe-Romo, J. Hunt, H. Furukawa, C. Kloeck, M. O'Keeffe and O. Yaghi, *J. Am. Chem. Soc.*, 2009, **131**, 4570.
3 N. Campbell, R. Clowes, L. Ritchie and A. Cooper, *Chem. Mater.*, 2009, **21**, 204.
4 G. Garberoglio and R. Vallauri, *Microporous Mesoporous Mater.*, 2008, **116**, 540.
5 J. Hunt, C. Doonan, J. LeVangie, A. Côté and O. Yaghi, *J. Am. Chem. Soc.*, 2008, **130**, 11872.
6 R. Tilford, S. J. Mugavero, P. Pellechia and J. Lavigne, *Adv. Mater.*, 2008, **20**, 2741.
7 A. Côté, H. El-Kaderi, H. Furukawa, J. Hunt and O. Yaghi, *J. Am. Chem. Soc.*, 2007, **129**, 12914.
8 H. El-Kaderi, J. Hunt, J. Mendoza-Cortes, A. Côté, R. Taylor, M. O'Keeffe and O. Yaghi, *Science*, 2007, **316**, 268.
9 R. Tilford, W. Gemmill, H.-J. Loye and J. Lavigne, *Chem. Mater.*, 2006, **18**, 5296.
10 A. Côté, A. Benin, N. Ockwig, M. O'Keeffe, A. Matzger and O. Yaghi, *Science*, 2005, **310**, 1166.
11 P. Kuhn, M. Antonietti and A. Thomas, *Angew. Chem., Int. Ed.*, 2008, **47**, 3450.
12 P. Makowski, J. Weber, A. Thomas and G. Goettmann, *Catal. Commun.*, 2008, **10**, 243.
13 P. Kuhn, A. Forget, D. Su, A. Thomas and M. Antonietti, *J. Am. Chem. Soc.*, 2008, **130**, 13333.
14 J. Schmidt, J. Weber, J. Epping, M. Antonietti and A. Thomas, *Adv. Mater.*, 2009, **21**, 702.
15 M. Tsyurupa and V. Davankov, *React. Funct. Polym.*, 2002, **53**, 193.
16 J. Ahn, J. Jang, C. Oh, S. Ihm, J. Cortez and D. C. Sherrington, *Macromolecules*, 2006, **39**, 627.
17 J. Germain, J. Hradil, J. M. J. Frechet and F. Svec, *Chem. Mater.*, 2006, **18**, 4430.
18 M. P. Tsyurupa and V. A. Davankov, *React. Funct. Polym.*, 2006, **66**, 768.
19 J. Germain, J. M. J. Frechet and F. Svec, *J. Mater. Chem.*, 2007, **17**, 4989.
20 H. R. Allcock, R. W. Allen, E. C. Bissell, L. A. Smeltz and M. Teeter, *J. Am. Chem. Soc.*, 1976, **98**, 5120.
21 H. R. Allcock, *Acc. Chem. Res.*, 1978, **11**, 81.
22 H. R. Allcock, U. Diefenbach and S. R. Pucher, *Inorg. Chem.*, 1994, **33**, 3091.
23 P. Mohanty and K. Landskron, *J. Mater. Chem.*, 2009, **19**, 2400.
24 K. Landskron, S. Schmid and W. Z. Schnick, *Z. Anorg. Allg. Chem.*, 2001, **627**, 2469.
25 Y. Sun and Y. Xia, *Science*, 2002, **298**, 2176.
26 M. C. Daniel and D. Astruc, *Chem. Rev.*, 2004, **104**, 293.
27 F. Kim, S. Connor, H. Song, T. Kuykendall and P. Yang, *Angew. Chem., Int. Ed.*, 2004, **43**, 3673.
28 X. Du and J. He, *J. Appl. Polym. Sci.*, 2008, **108**, 1755.
29 Z. Meng, C. Xue, Q. Zhang, X. Yu, K. Xi and X. Jia, *Langmuir*, 2009, **25**, 7879.
30 S. Kothai Nayaki and M. Swaminathan, *Spectrochim. Acta, Part A*, 2002, **58**, 2931.
31 N. Rajendiran and M. Swaminathan, *Bull. Chem. Soc. Jpn.*, 1995, **68**, 2797.
32 A. Van Blaaderen, J. Van Geest and A. Vrij, *J. Colloid Interface Sci.*, 1992, **154**, 481.

